

In-Flight Boundary-Layer Transition Measurements on a Swept Wing

Anwar Ahmed*

Texas A&M University, College Station, Texas

William H. Wentz†

Wichita State University, Wichita, Kansas

and

R. Nyenhuis‡

Cessna Aircraft Company, Wichita, Kansas

Flight tests were conducted at three different altitudes to detect transition on a smoothed test region of a swept-wing business jet wing using surface hot-film sensors and sublimating chemicals. Strong influence of sweep angle on transition location was observed when the aircraft was flown at some sideslip conditions to simulate changes in effective wing sweep angle. No effects of engine noise on transition were measured when different engine power settings were used. Flight instrumentation and ground data analysis techniques are described. Correlation was obtained between the hot-film sensor signals and sublimating chemicals for transition detection. Crossflow vortices were observed for one flight condition. Results of analyzed data for various flight-test conditions are presented.

Nomenclature

c = wing chord
 M_{CAL} = calibrated Mach number
 Λ = angle wing sweep

Introduction

THE desirability of achieving the low drag levels associated with laminar boundary-layer flow is unquestioned and has been the subject of research extending over many years. For the past three decades, however, it was generally conceded that riveted aluminum fabrication used for all large-volume production airplanes produced surface roughness that caused early transition and, therefore, precluded laminar flow. Increasing fuel costs and the introduction of composite materials as potential aircraft primary fabrication material have resulted in renewed interest in the possibilities of natural laminar flow, since these new fabrication techniques will make possible the attainment of smoother surfaces.

Although the process of laminar boundary-layer stability has been the subject of intensive research spanning decades, it is not yet completely understood. Several analytical techniques have been used for determining transition location. Most of these methods assume two-dimensional perturbations in the form of waves (Tollmien-Schlichting waves) propagating in the streamwise direction. The solution of the equations of classical stability theory yields constant amplification factor boundaries as a function of pressure gradient, frequency of disturbance, and Reynolds number. Schlichting¹ used a family of laminar velocity profiles based on Pohlhausen's approximate method to calculate curves of neutral stability and found that the stability was greatly dependent on the pressure gradient and Reynolds number. It was also revealed that profiles with inflections which arise in the two-dimensional case as a result of the adverse pressure gradient, are much less stable than the profiles without inflections. The stability theory as developed by Schlichting and Ulrich provided the neutral stability boundary, but not the transition location.

Smith² furthered this work by correlating transition location with a disturbance amplification factor and found that the transition occurred for a wide variety of cases when the value of the amplification factor integrated between the point of instability and the point of transition was equal to e^9 . Smith's hypothesis is backed by many experiments.

Boundary-layer instability in a two-dimensional flow such as an upswept wing is related to Tollmien-Schlichting waves. These waves are amplified if the Reynolds number is large or if an inflection is present due to the adverse pressure gradient. Instability is also caused by the amplification of disturbances present in the freestream. When the wing is swept forward or back, the stability problem is aggravated. Two problems associated with the sweep are the crossflow inflectional instability and the spanwise turbulent contamination of the wing leading edge along the attachment line.

The boundary-layer profiles on a swept wing have a crossflow component. Since the crossflow component has zero velocity at the surface and asymptotically approaches zero at the outer edge of the boundary layer, every crossflow profile must contain an inflection, irrespective of the chordwise

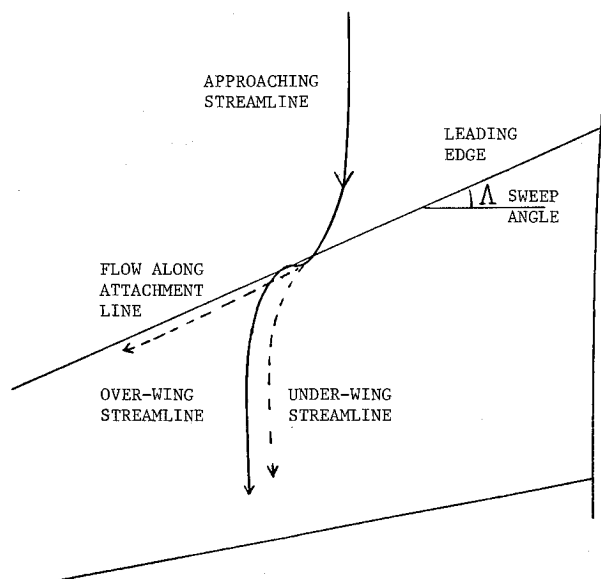


Fig. 1 Streamlines in the leading-edge region of a swept wing.

Received Sept. 29, 1988; revision received April 12, 1989. Copyright © 1989 American Institute of Aeronautics and Astronautics, Inc. All rights reserved.

*Assistant Professor, Aerospace Engineering Department. Member AIAA.

†Distinguished Professor, Aeronautical Engineering Department. Member AIAA.

‡Aerodynamicist, Cessna Wallace Division. Member AIAA.

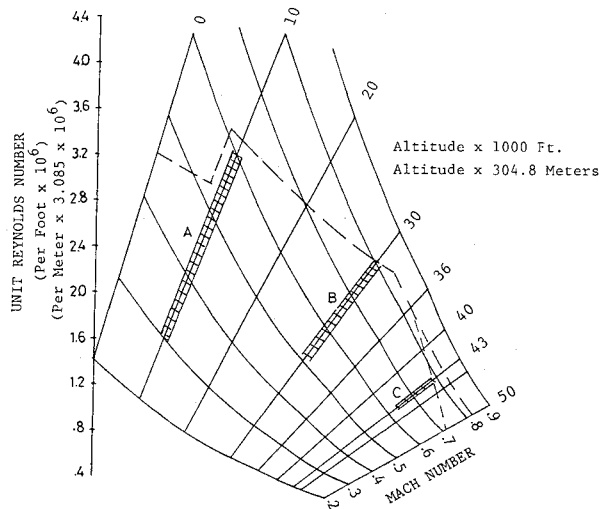


Fig. 2 Flight envelope of Cessna model 650 business jet.

pressure gradient. Inflectional instabilities are more powerful than the viscous instabilities. Thus, the boundary layers with crossflow are expected to be much less stable than two-dimensional boundary layers. Another complicating factor related to the crossflow is the formation of a discrete array of vortices running parallel to the potential-flow streamlines. Formation of these vortices has been reported by Gregory et al.³ and Bolz et al.⁴ for a certain combination of airfoil geometry, sweep, and Reynolds number. Skin-friction levels associated with these vortices have not been established.

Figure 1 shows the streamline pattern in the leading-edge region of a swept wing. It can be seen that the stagnation line in the two-dimensional flow has been replaced with an "attachment line" that has a nonzero velocity component in the spanwise direction. As a result, turbulence generated by the disturbances at the wing-body junction or by any other supercritical roughness element may be convected spanwise along the attachment line. This phenomenon associated with the swept wing is known as turbulent contamination of the leading edge. A complete treatment of the attachment line can be found in Ref. 5.

Only limited analysis has been conducted for boundary-layer stability on swept wings. Furthermore, the question of the amplification required for transition to occur beyond the instability point remains unanswered for the swept wings.

The present project was undertaken with the following objectives: 1) to develop instrumentation to determine the extent of natural laminar flow and transition location on a swept wing at various Mach number, altitude, and Reynolds number combinations; 2) to determine the effects of wing sweep on transition; 3) to evaluate laminar flow in a realistic flight environment and in the absence of typical wind-tunnel turbulence; 4) to determine whether engine acoustic interference will cause premature transition; and 5) to correlate transition locations with the local waviness of the wing surface.

Experimental Procedure

A Cessna 650 Citation III business jet with a wing sweep of 27.23 deg was used as a testbed aircraft for this flight-test program.

Flight-test conditions with various Mach numbers at the three altitudes of 3048 m (10,000 ft), 9144 m (30,000 ft), and 13,106 m (43,000 ft) were selected to represent the widest possible range of Reynolds numbers. These flight-test conditions are shown on the flight envelope of the aircraft in Fig. 2 and are marked as A, B, and C.

All conditions were flown straight and level. For selected cases, sideslips of a few degrees to the left and to the right were also flown to observe the influence of effective wing sweep on transition.

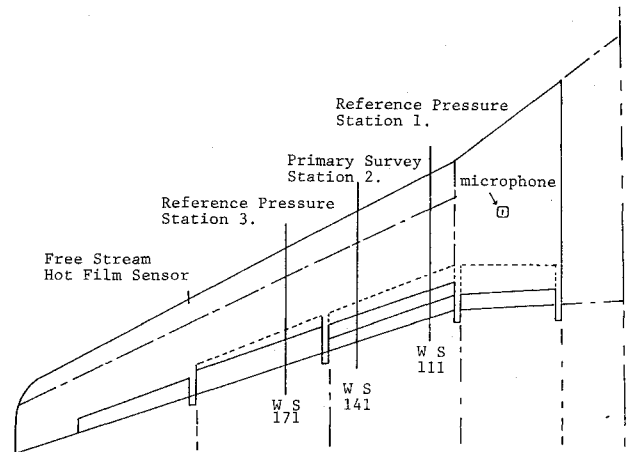


Fig. 3 Details of measurement stations on the swept wing.

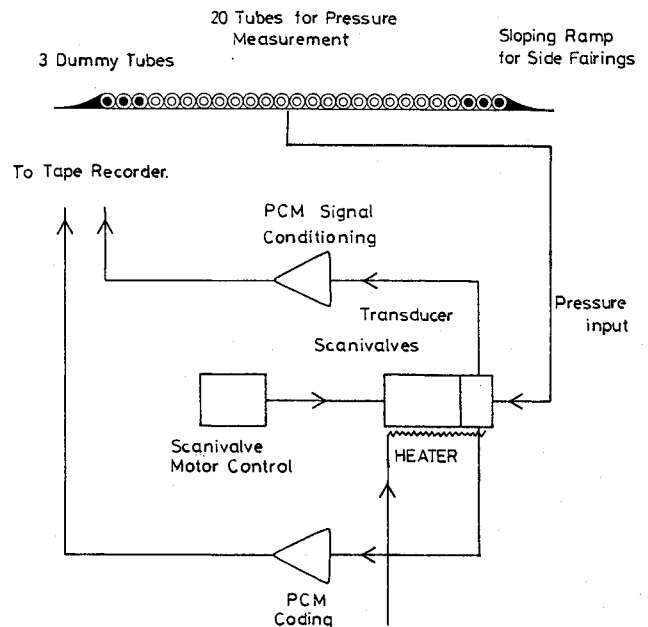


Fig. 4 Details of wing surface pressure measurement system.

To study the effects of engine noise on the boundary layer, selected conditions were flown with different power settings on the left and right engines.

Preparation of the Wing Section

In order to measure transition accurately, a region of the wing between wing stations (WS) 171 and 111, which was relatively free from extraneous aerodynamic interference, was selected. (A wing station is the distance in inches measured from the aircraft centerline). This region, as shown in Fig. 3, was covered with fiberglass and filled and smoothed to minimize surface roughness due to screw heads, rivets, and joints. This fiberglass layer provided additional thermal insulation between the hot-film sensors and the wing skin.

Since waviness of the wing surface could cause premature transition, plaster splashes of both the upper and lower wing surfaces between WS 141 and 144 were made, and the actual profile and waviness were measured accurately using a machine shop long-bed planer and precision micrometers. More details can be found in Ref. 6.

To maximize the contrast between the wing surface and the white sublimating chemical, the test region of the wing was painted with low-gloss black paint.

Pressure Measurement

Pressure measurements were made at WS 111, 144, and 171. Static pressures were measured with the help of pressure belts glued to the surface of the wing at the three stations. Each tube was 2.54 mm o.d. and 0.787 mm i.d. The average length of the pressure belts was 5.5 m. Each pressure belt had three dummy tubes attached to each side, together with a sloping ramp for side fairings.

The belts were routed inboard through the flap cavity to the fuselage where they were attached to the three 48-port multiple scanners (scanivalves), each with one transducer and signal conditioner. The temperature of the scanivalves was controlled by auxiliary heaters (Fig. 4). Pulse code modulation (PCM) encoding was used for pressure port identification and recording. Each pressure transducer was referenced to the aircraft boom static pressure, which was also recorded to measure any possible zero drift during testing.

Pressure surveys on WS 111 and 171 were used to find the correlation between the pressure distributions at these stations and the stations where the surface hot-film sensors were later installed for transition measurement. A second objective of measuring pressures at three stations was to see if the isobars were reasonably straight across this portion of the wing.

Transition Measurement Techniques

Transition may be detected by a variety of methods: sublimation of chemicals and color changes of liquid crystals applied to the surface, boundary-layer profile measurements, surface microphones, and surface hot-film anemometry. For in-flight transition measurements, two experimental techniques were used. These techniques were tested earlier on a Cessna P-210 airplane⁷ and are described next.

Sublimating Chemicals

Sublimating chemicals provide visual information about the location of transition and also indicate whether the transition has been caused by surface roughness or contamination of the surface with insects or dirt.

This technique makes use of the fact that sublimation rates are strongly related to boundary-layer convection. Therefore, turbulent boundary layers have higher sublimation rates than laminar ones. With a proper material and application rate, the aircraft can be flown for 15 to 30 min under steady-state conditions at a given altitude before a transition front is established by sublimation in the turbulent region. During this time, photographs of the visible parts of the wings are taken. Additional photographic records of both the upper and lower surfaces are made on the ground after landing. A typical flow pattern as seen after the sublimation of chemicals is shown in Fig. 5. Transition triggered by an insect strike or due to a supercritical roughness element is observed in the form of a turbulence wedge. This technique is nonintrusive, but it is limited to one Mach number and altitude per flight. Care must be taken in matching the sublimating chemical to the pressure and temperatures at a given altitude, so that the local pressure will be near the vapor pressure of the sublimating chemical.⁸

In applying sublimating chemicals for a visual record of transition, the wing surface was wiped with a lightly dampened cloth to remove dust particles. A premixed solution

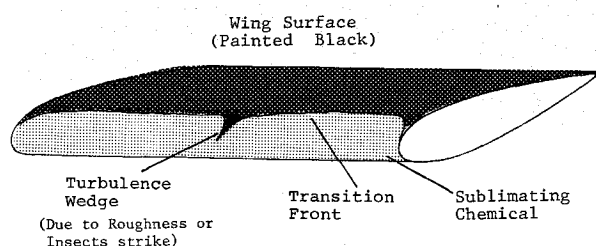


Fig. 5 Flow pattern due to sublimating chemicals.

of one part by volume of acenaphthene to eight parts of trichloroethane was sprayed on the wing. The trichloroethane evaporated, leaving behind a thin film of acenaphthene residue on the wing. The wing surface was sprayed several times to achieve a film of reasonable thickness. After each spray coat, the surface was brushed lightly with a soft brush and cheesecloth to ensure a "clean" surface. Finally, the area was hand-rubbed using surgical gloves and light pressure. This technique smooths and compresses the chemical, slowing initial sublimation rates so that stable flight conditions can be established before major sublimation occurs.

Hot-Film Anemometry

The constant-temperature hot-film anemometer utilizes an amplifier to maintain a constant sensor temperature. The basic anemometer circuit to which a hot-film sensor of a given operating resistance is attached consists of a quarter bridge. The bridge is balanced and adjusted through a variable control resistor. The sensitivity of the bridge for turbulence measurement depends directly on the overheat ratio, which is the ratio for the sensor operating temperature to the ambient temperature.

The overheat ratio is set by setting the value of control resistance greater than the sensor operating resistance. Setting of the overheat ratio greater than unity offsets the bridge balance, which causes the bridge to operate with increased voltage across the anemometer. This increase in voltage increases the probe temperature above the surrounding. The anemometer tends to maintain this overheat by regulating the bridge voltage to keep the probe temperature constant. Fluctuation of the bridge voltage required to maintain constant temperature is a measure of the unsteadiness of the flow over the sensor.

Temperature Compensation

With an increase in altitude, ambient temperature falls at about 3.5°F/1000-ft alt. Since the hot-film sensors are exposed to ambient conditions, any decrease in ambient temperature results in a higher overheat ratio, thus requiring an increase in power input to the sensors to maintain constant temperature. This response would falsely indicate increased activity in the boundary layer, even at constant velocity. Another problem associated with the increase in overheat is the higher power requirements, which are limited by the power inverters of the aircraft.

To overcome this problem, a temperature compensation system was designed and installed in the tail cone of the aircraft. This unpressurized area of the airplane has a large ram air scoop, which provided air temperatures within a few degrees of ambient. The compensation system was connected to the control leg of the anemometer bridge, and the overheat was set with additional potentiometers. With this system, the ane-

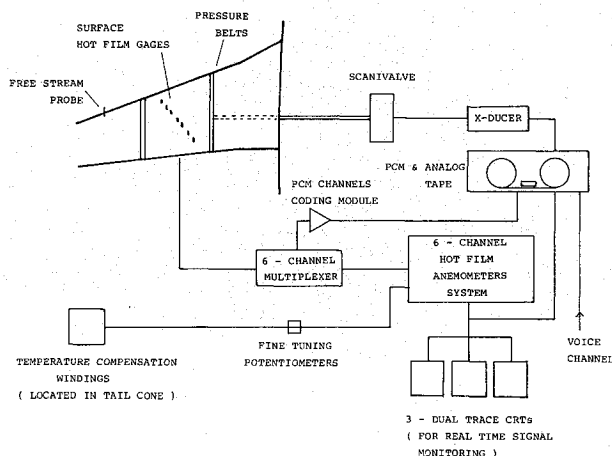


Fig. 6 Instrumentation for transition measurement.

moments were tuned only once on the ground and no further adjustments were required at any other altitude. Therefore, the system as modified with temperature compensation operated at a constant overheat ratio at all altitudes.

After the initial pressure measurement flights, the pressure belt on the middle portion was removed and the wing surface was cleaned for the installation of hot-film sensors. A total of 29 Micro Measurements MM-ETG-50Ω hot-film sensors with an operating resistance of 50 Ω were installed—15 on the upper surface and 14 on the lower surface. The first two sensors on both the upper and lower surfaces were installed at 2.5 and 5% of the chord. The remainder were installed at 5% increments. The sensors were staggered 15 deg inboard to protect each sensor from the wake of the sensors ahead. A pair of 28 SWG enameled copper wires were used to connect each sensor with one of the five anemometers inside the airplane through a mechanical multiplexing system. The lead wires were twisted to minimize electrical interference. The multiplexing system was designed so that a sequence of any five consecutive sensors could be monitored, PCM encoded, and provided a continuity check for each sensor. A total of six TSI model 1050 A anemometers were used. Five anemometers were used for transition measurements, and the sixth anemometer channel was dedicated to the freestream probe. A standard conical tip probe (TSI model 1230) was installed ahead of the wing leading edge for freestream turbulence monitoring.

Three dual-trace oscilloscopes were used for in-flight monitoring of the six anemometers. The sensor multiplexer positions were PCM coded. The anemometer signals were recorded on an onboard Honeywell model 5600-C analog tape recorder on intermediate band frequency modulation channels. A separate voice channel was used for miscellaneous flight information and hot-film signal interpretation from the oscilloscopes' traces. A schematic of the instrumentation involved shown in Fig. 6.

Noise Measurement

In addition to the hot-film data, a microphone assembly consisting of a B&K condenser microphone cartridge type 4133 with nose cone UA 0386 was installed on a modified pitot-tube support to record the sound from the engine to which the wing boundary layer was exposed. The microphone was located midchord at WS 96. The microphone signals were recorded directly as analog data.

Data Analysis

After each flight, the recorded tape was played back on the ground to obtain the strip-chart output of the aircraft flight parameters, such as altitude, angle of attack, indicated and calibrated airspeeds, ambient conditions, and time code. The strip chart was studied carefully and the time segments of the

most steady flight conditions were selected. These segments of the signals of the hot-film sensors, pressures, and microphone were later processed in the time domain and frequency domain.

For the time-domain analysis, Cessna ground processing equipment was used. The ground analysis schematic is shown in Fig. 7. The analog data tape was played back into a PDP 11/40 system, where, with the help of a time decoder/translator, PCM decoder, and real-time monitor, these data were segmented into 20-ms data blocks, digitized, and stored on a hard disk. For highest possible resolution, an available system sampling rate of 50 kHz was used. All signals were ac coupled. Statistical analysis on the stored data was performed later using the GenRad operating system Time Series language.

The frequency-domain analysis of the signals was performed at Wichita State University using the HP 5423A Fourier analyzer. With the high-resolution autospectrum option available in the analyzer, a frequency resolution of 12.5 Hz was achieved over a frequency bandwidth of 6.4 kHz. For the statistical stability of the random signals, 20 ensemble averages were taken for each hot-film signal at each flight condition.

Interpretation of Transition Data

Three methods of interpreting the data of the hot-film gauges were used to determine the transition location on the wing.

1) Time History: Typical time records of the signals of a series of hot-film sensors are shown in Fig. 8. Laminar signals are relatively smooth. Prior to transition, the ac component of the signal shows "turbulence spikes," an indication of higher activity and an intermittent increase in signal voltage. Immediately after transition, the flow tends to retain infrequent periods of laminar flow, which appear as "negative" or "laminar spikes." At a distance farther downstream of the transition location, the flow becomes completely turbulent.

2) Root-mean-square of Perturbations: After statistical analysis of the signals, one can determine the transition location by examining the rms value of the signal. A plot of rms values of the signals is shown in Fig. 9. Proceeding downstream, the hot-film sensor exhibiting the first major peak in rms value is taken as the one indicating transition.

3) Power Spectral Density: The third method of determining transition is through frequency-domain analysis. The power

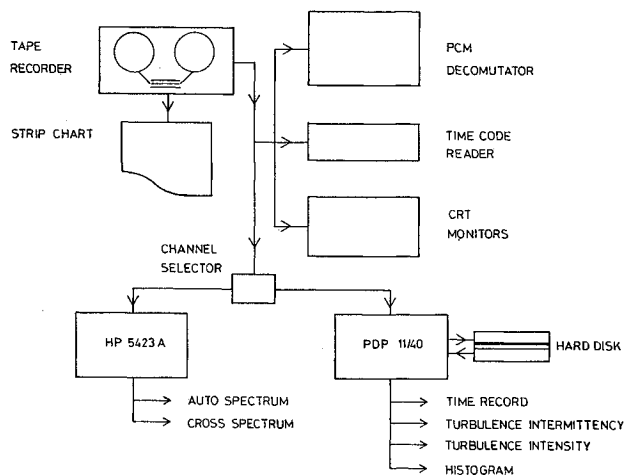


Fig. 7 Ground data processing layout.

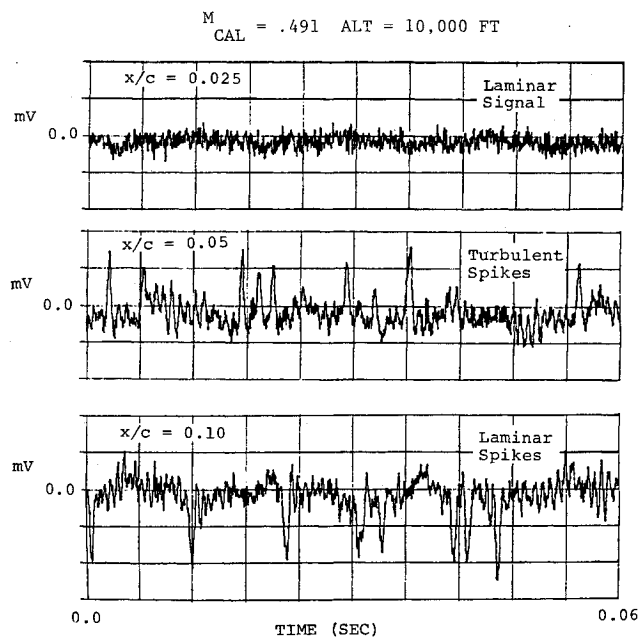


Fig. 8 Time records of hot-film sensor signals showing laminar and turbulent spikes.

Table 1 Summary of measured transition locations for flight-test program

Transition location, % X/C							
No.	Altitude, ft (m)	M_{CAL}	Wing surface	In-flight monitoring (time records), %	Ground analysis		Sublimating chemicals, %
					Time-domain rms, %	Frequency-domain psd, %	
1	10,000	0.295	Upper	5	5	5	5
2		0.295	Lower	10	10	10	10
3	(3048)	0.491	Upper	10	5-10	5-10	5-10
4		0.538	Upper	5	5	5	
5	30,000	0.441	Upper	15	15	15	
6		0.441	Lower	10-15	10-15	10-15	
7	(9144)	0.631	Upper	10	NC	10	
8		0.631	Lower	10	10	10	
9		0.678	Upper	15	15	15	
10		0.724	Upper	10	10	10	
11		0.771	Upper	5	5	5	
12		0.771	Lower	5	5	5	
13		0.798	Upper	5	5	5	
14	43,000	0.581	Upper	10	10	10	
15		0.581	Lower	35	35	35	
16	(13,106)	0.682	Upper	10	10	10	
17		0.682	Lower	30	30	30	

NC: No correlation was obtained (noisy reproduced signal).

spectra of a laminar signal, transitional signal, and a completely turbulent signal are given in Fig. 10. The transition signal shows a much higher power spectral density at the lower end of the frequency spectrum than either a fully laminar or turbulent signal.

The advantage of frequency-domain analysis is that system noise that may appear to be dominating the signal in the time domain usually appears as a single peak or spike in the frequency domain and, therefore, can be eliminated by suitable filtering.

Results and Discussion

A summary of transition locations measured during the flight-test program is given in Table 1.

Comparing the measured upper surface transition locations for each flight condition with the corresponding pressure distributions (Fig. 11), it was observed that transition occurred behind the minimum pressure point. This indicates that the transition was caused by a combination of normal amplification of the Tollmien-Schlichting waves in the regions of adverse pressure gradients coupled with crossflow, and not due to external disturbances such as engine noise, structural vibrations, surface waviness, and/or roughness. If transition had been caused by these effects, it would have occurred at locations ahead of the minimum pressure points. This pattern was consistent for the entire range of Reynolds numbers at all altitudes.

On the lower surface, it was observed that favorable pressure gradients existed up to 50% of the chord in some

cases, but the transition location remained near the leading edge. This is an indication that the crossflow instability was responsible for the transition.

The surface waviness based on actual dial gauge readings and a nine-point running average are presented in Fig. 12. It was found that the actual waviness measured was considerably below the criterion for the maximum allowable height for the single wave.⁹ It must be noted that these measurements were made with the aircraft on the ground and, although this wing is relatively stiff, contours may be different during flight due to aerodynamic loading.

To investigate possible effects of engine noise on transition, the engine on the left instrumented wing of the airplane was throttled back to 70% of full rpm, and the right engine was advanced as necessary to maintain speed. The aircraft was trimmed for zero sideslip with asymmetric thrust. This condition was flown at 9144 m and a calibrated Mach number of 0.631. The power spectra of the microphone signals before and after engine rpm reduction are shown in Fig. 13. The spectra are quite similar. This indicates that either the noise from the various aircraft boundary layers dominates the engine noise, the microphone forebody generates noise that dominates engine noise, or the wing boundary-layer noise is unaffected by engine noise.

The hot-film anemometers indicated no changes associated with engine power settings. To further validate the inference that engine noise was not causing transition, power spectra of the hot-film sensor that indicated transition at full engine power setting and after a reduced engine power setting are presented in Fig. 14. No noticeable differences can be seen. This provides conclusive evidence that engine noise was not responsible for observable changes in transition location for the configuration and flight condition tested.

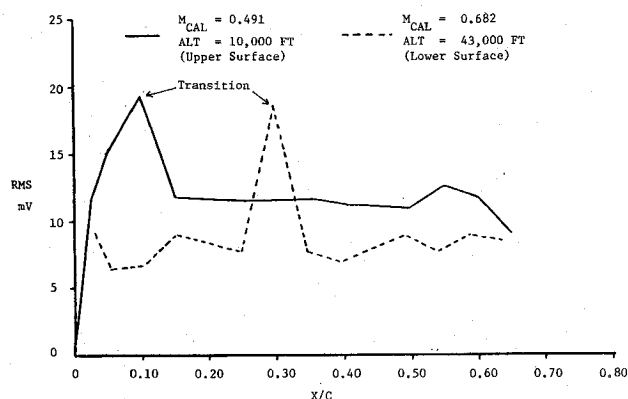


Fig. 9 Root-mean-square value of surface hot-film signals for two flight conditions.

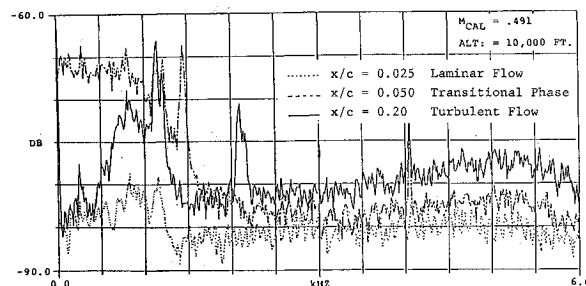


Fig. 10 Power spectra of laminar, transitional, and completely turbulent signals.

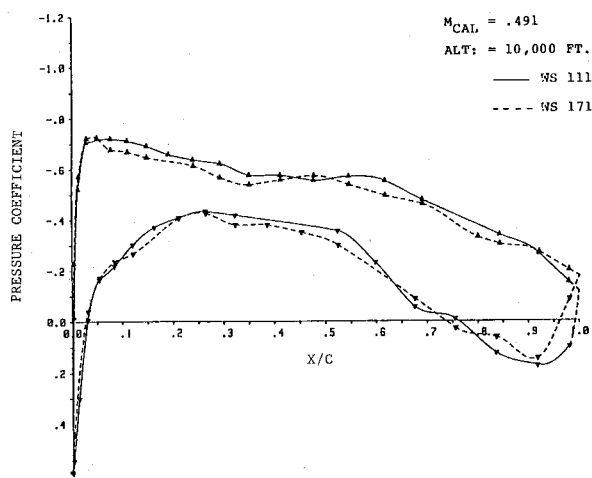


Fig. 11 Surface pressures at two wing stations.

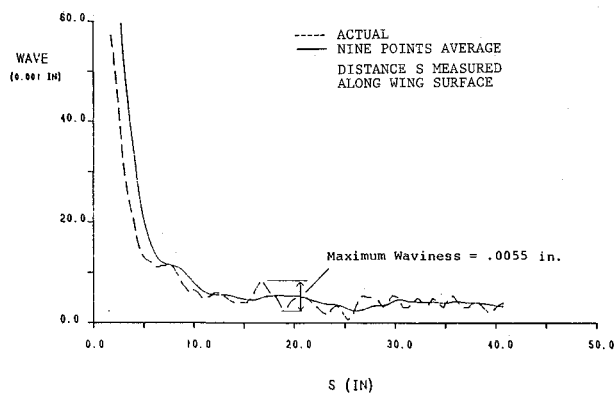


Fig. 12 Surface waviness of the wing at WS 150 (upper surface).

Sublimating chemicals were used to obtain correlation between the transition locations measured by the hot-film sensors and the sublimating chemicals. Two flight conditions at an altitude of 3048 m were selected. They were made at calibrated Mach numbers of 0.491 and 0.295, respectively.

After the pattern was fully developed on each flight, photographs were taken during flight. Transition location was measured by comparing the chemical pattern with white stripes painted on the wing surface at increments of 5% chord between WS 111 and 171. After the aircraft landed, additional photographic records were made on the ground. The chemical remained visible on the wing for up to 2 h after landing, indicating the insensitivity of the chemical to short-duration changes in temperature, pressure, and velocity.

Close ground examination of the chemical patterns from the Mach 0.491 flight revealed parallel streaks, indicating small, discrete crossflow vortices near the wing leading edge. These vortices are shown in Fig. 15. It was observed that the number of these discrete vortices was approximately 7/cm; these vortices were oriented parallel to the potential-flow stream line. There was no evidence of such vortices for the second flight flown at Mach 0.295. In the presence of surface contamination due to insects, bugs, or chemical lumps, turbulent wedges are formed and can be seen in sublimation photo records.

The chemicals did not show any indication of turbulent contamination of the leading edge along the attachment line. This is in accordance with predictions made using an attachment line boundary-layer momentum thickness Reynolds number criterion.¹⁰

In addition to straight and level conditions, sideslips of about 4 deg nose right and left were flown at 9144 m at a calibrated Mach number of 0.631. Power spectra indicate that the transition location moved forward from 10 to 5% chord when

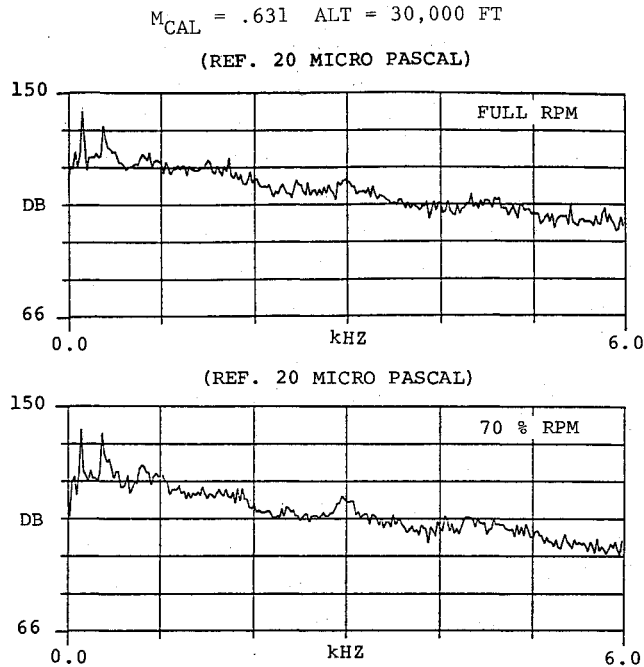


Fig. 13 Power spectra of microphone signals at different power settings.

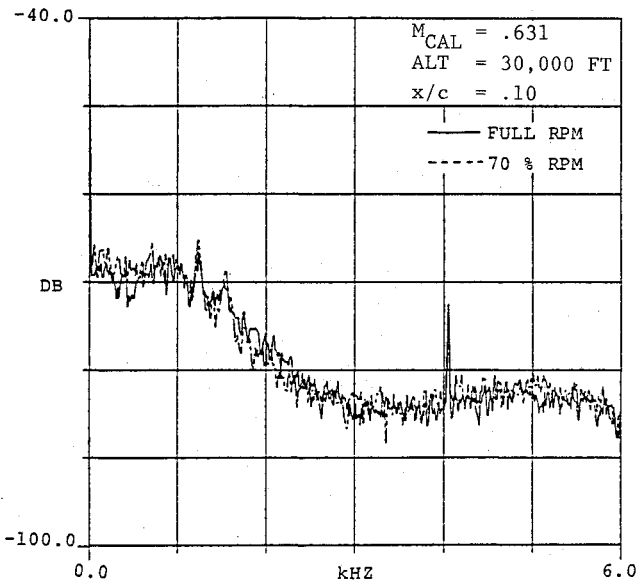


Fig. 14 Power spectra of the sensor indicating transition at full and 70% rpm.

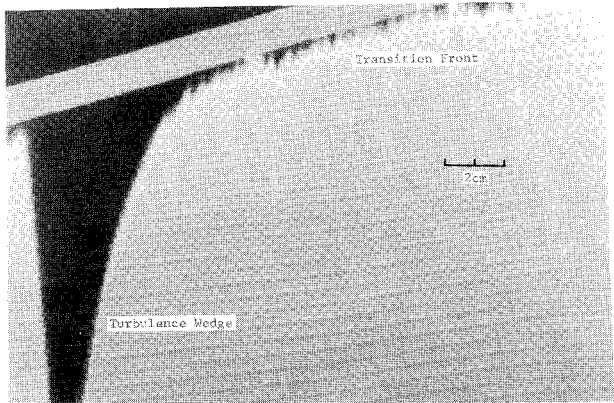


Fig. 15 Close-up of a sublimation chemical photograph showing crossflow vortices.

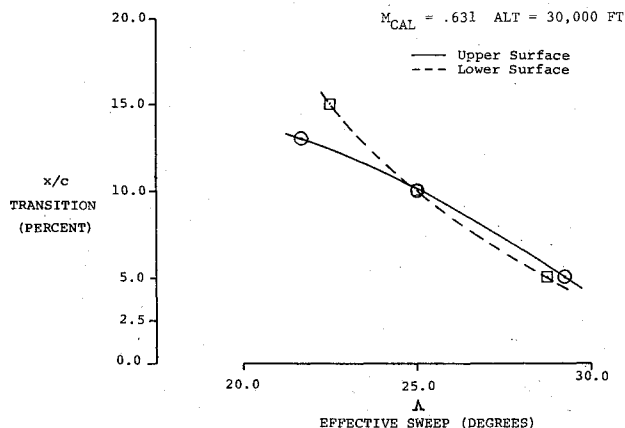


Fig. 16 Effect of wing sweep on transition location.

effective sweep was increased. A sideslip to decrease effective sweep had an opposite effect.

On the lower surface, an increase in sweep moved the transition location forward to 5 from 10% chord, and a decrease in effective sweep moved the transition from 10 to 15% chord.

The changes in transition location with the change in effective sweep are shown in Fig. 16. This figure illustrates that transition is influenced strongly by sweep.

Conclusions

1) Temperature-compensated hot-film anemometry instrumentation developed for this research successfully met its objectives for measuring transition locations on the wing surface over a wide range of subsonic Mach numbers and at altitudes up to 13,106 m. Hot-film measurements correlated with limited sublimating chemical tests.

2) Identification of transition location from peak rms signals correlated well with in-flight time-history observations.

3) Identification of the transition location from the psd of the hot-film signals correlated well with the time-history observations of the conditions analyzed.

4) No evidence of turbulent contamination of the wing leading edge was found.

5) Measured surface waviness of the wing surface was less than the critical values for the onset of transition.

6) Sideslip tests revealed that an increase in sweep moves the transition location forward, and a reduction in effective sweep delayed the transition.

7) No measurable changes in transition location or noise levels were observed as a result of changes in engine rpm.

8) Discrete, small-scale, crossflow vortices were observed in the sublimating chemical pattern for Mach 0.491 flight at 3048 m. These observations indicated that crossflow vortices may be responsible for "premature" transition on swept wings.

Acknowledgment

This research was conducted under NASA Langley Grant NAG1-104, monitored by Dana Morris and Dr. Bruce Holmes.

References

- ¹Schlichting, H., *Boundary Layer Theory*, McGraw-Hill, New York, 1979.
- ²Smith, A. M. O., "Transition, Pressure Gradient and Stability Theory," *Proceedings of 9th International Congress of Applied Mechanics*, Brussels, Vol. 4, 1957, pp. 234-244.
- ³Gregory, N., Stuart, J. T., and Walker, W. S., "On the Stability of Three Dimensional Boundary Layers with Application to the Flow Due to Rotating Disk," *Boundary Layer Effects in Aerodynamics, NPL Proceedings*, Philosophical Transactions of the Royal Society, London, Vol. 248, 1955, pp. 155-199.
- ⁴Boltz, F. W., Kenyon, G. C., and Allen, C. Q., "Effects of Sweep Angle on the Boundary Layer Stability Characteristics of an Untapered Wing at Low Speeds," NASA TN D-338, Oct. 1960.
- ⁵Poll, D. I. A., "The Development of Intermittent Turbulence on a Swept Attachment Line Including the Effects of Compressibility," *Aeronautical Quarterly*, Vol. 34 (Pt. 1), Feb. 1983, pp. 1-23.
- ⁶Ahmed, A., "Natural Laminar Flow Flight Experiments," Ph.D. Dissertation, Aeronautical Engineering Dept., Wichita State Univ., KS, 1984.
- ⁷Wentz, W. H., "Instrumentation for Flight Measurement of Boundary Layer Transition," Paper presented at AIAA Technologyfest, Wichita, KS, Nov. 1983.
- ⁸Holmes, B. J., Obara, C. J., and Yip, L. P., "Natural Laminar Flow Experiments on Modern Airplane Surface," NASA TP-2256, June 1984.
- ⁹"Final Report on Laminar Flow Control Demonstration Program," Northrop Corp., Hawthorne, CA, NOR 67-136, June 1967.
- ¹⁰Beasley, J. A., "Calculation of the Laminar Boundary Layer and Prediction of Transition on a Sheared Wing," British Aeronautical Research Council R&M 3787, Oct. 1973.